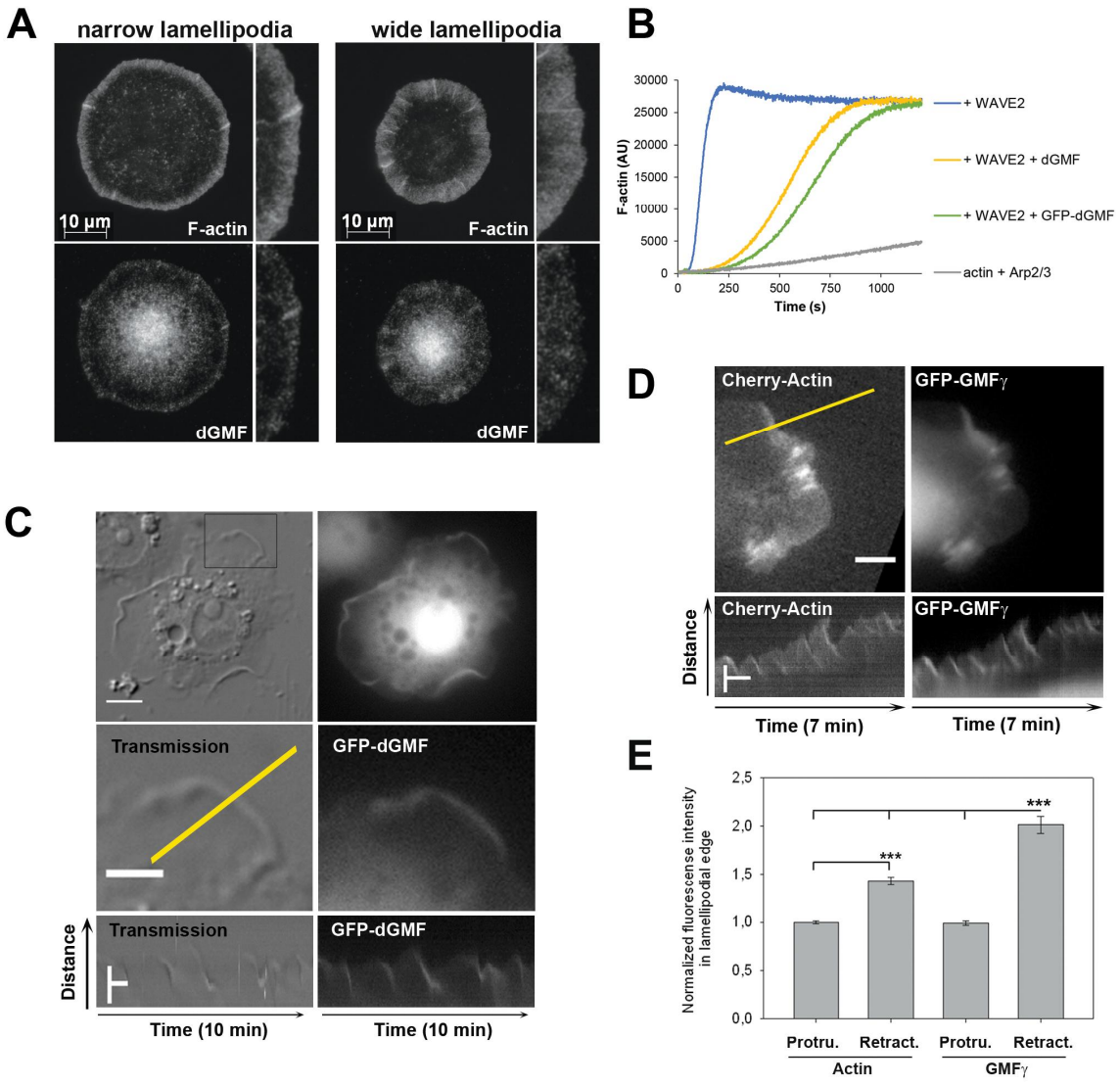

Figure S1. Localization of GMF in cultured *Drosophila* and mammalian cells. Related to Figure 1.

(A) The localization of endogenous dGMF at lamellipodial edge in *Drosophila* S2R+ cells plated on ConA. Please note that localization of dGMF correlates inversely with the width of F-actin rich region of the lamellipodia. dGMF was detected with an antibody and F-actin with phalloidin. (B) Inhibition of Arp2/3 complex-mediated actin assembly *in vitro* by GFP-tagged *Drosophila* GMF (dGMF). Reactions contained 2 µM actin monomers (5% pyrene-labeled), 20 nM bovine Arp2/3 complex, 50 nM human WAVE2 GST-VCA, and 2 µM dGMF or GFP-dGMF. (C) Time-lapse images of GFP-dGMF at lamellipodia in *Drosophila* S2 cells. For studying the dynamics of GFP-dGMF at the cell edge over time, a line was drawn perpendicular to the cell surface (indicated by yellow line in the middle panel). In a kymograph below, each frame of a time-lapse movie along the line is shown along the y-axis

whereas the x-axis represents time (total 10 min). GFP-dGMF appears to become enriched at the lamellipodial edge specifically at the time of retraction. Bars, 10 μm (and 5 μm in higher magnification images) and 1 min in x-axis of the kymograph. **(**D) Dynamic localization of Cherry-Actin and GFP-GMFγ in mouse melanoma B16.F1 cells. Actin localizes to the lamellipodial edge both during its protrusion and retraction phases, whereas GFP-GMFγ becomes concentrated at the lamellipodium only during the retraction phase. Bars, 5 μm (cell image and y-axis of kymograph) and 1 min in x-axis of kymograph. (E) Quantification of the fluorescence intensities of Cherry-Actin and GFP-GMFγ at lamellipodial edge during protrusion and retraction phases. The fluorescence intensity during protrusion is normalized as 1. (Data collected from 4 movies, 11 kymographs, 74 protrusions and 68 retractions.) *** $p < 0.001$ Students T-test. Data are represented as mean ± SEM.

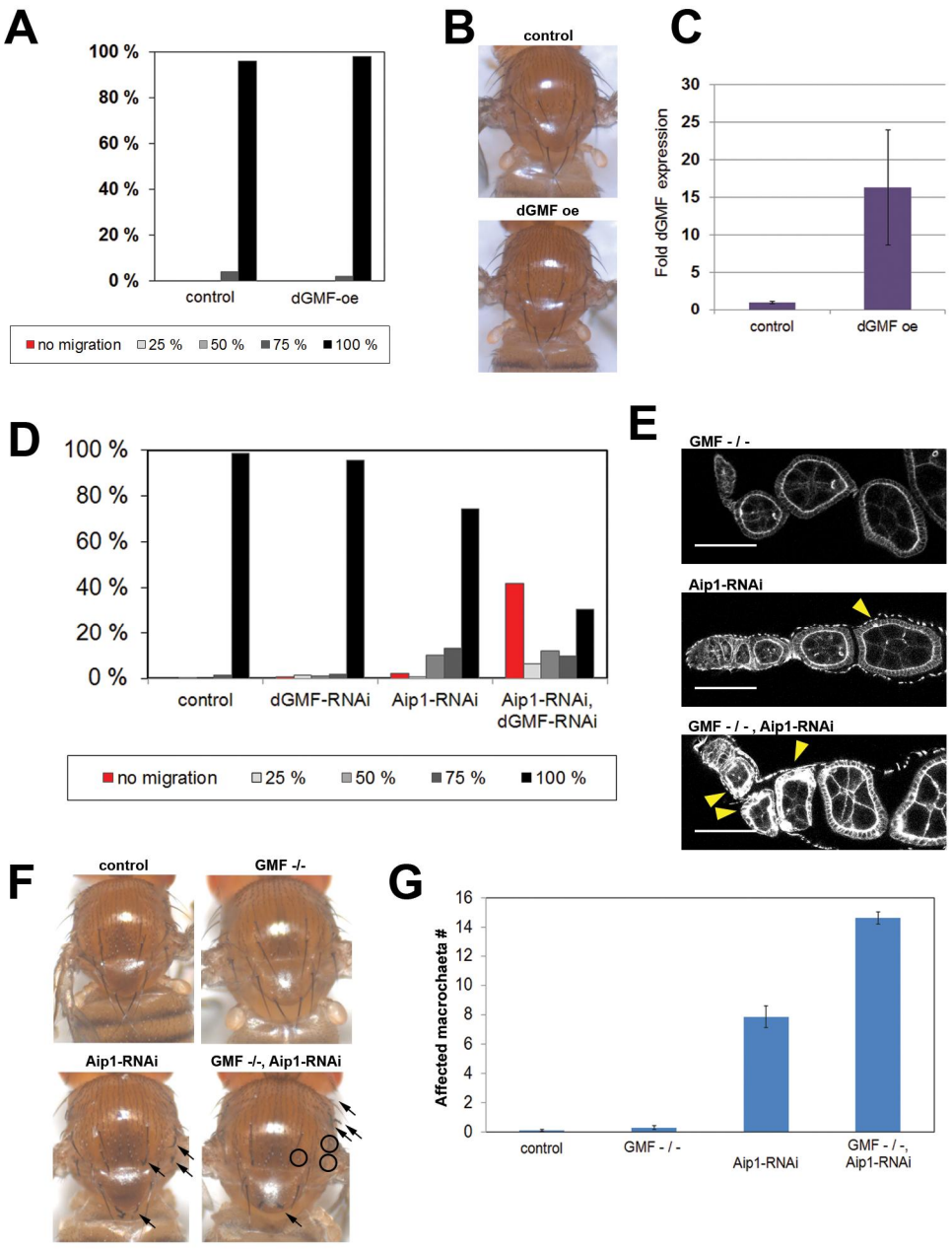

Figure S2. Genetic interactions between dGMF and Aip1 confirmed using an independent Aip1-RNAi line and by RNAi silencing of dGMF.

Related to Figure 2.

(A-C) Ubiquitous over-expression of dGMF in flies did not cause detectable border cell migration delays in stage 10 (panel A) or phenotypes in bristles (panel B). (C). Quantitative RT-PCR demonstrated >15-fold higher GMF mRNA expression in mutant flies compared to control flies. Data are represented as mean ± SD. Genotypes used for A-C were: control (+/+; +/+; +/Tub-Gal4) and dGMF-oe (+/+; +/cg5869 EPG2885; +/Tub-Gal4). (D) Quantification of border cell migration delays in stage 10 egg chambers (as in Figure 2F) upon Aip1 silencing and dGMF silencing. Genotypes are: c306Gal4/+ (control), c306Gal4/+; UAS-

GMF-RNAi-kk/+ (dGMF-RNAi), c306Gal4/+; UAS-Aip1-RNAi kk/+ (Aip1-RNAi) and c306Gal4/+; UAS-Aip1-RNAi kk/ UAS-GMF-RNAi-kk (Aip1RNAi, dGMF-RNAi). N > 200. (E) Confocal images of developing egg chambers showing F-actin accumulation in the follicular epithelium. Simultaneous silencing of Aip1 and dGMF results in strong accumulation of F-actin in these cells. All confocal images were obtained using identical microscope settings. (F) Genetic interaction between dGMF and Aip1 was also detected in development of bristles. Deformed (arrows) or missing (circles) macrochaeta are indicated on the right side of the thorax. (G) Quantification of deformed or missing macrochaeta from thorax was performed by light microscopy. Data are represented as mean ± SEM. N=20. Genotypes for D, E, F and G are: c306Gal4/+ (control), c306Gal4/+; gmf^{1}/gmf^{1} (GMF -/-), c306Gal4/+; +/+; UAS-Aip1-RNAi GD/+ (Aip1-RNAi) and c306Gal4/+; gmf^{1}/gmf^{1}; UAS-Aip1-RNAi GD/+ (GMF -/-, Aip1-RNAi).

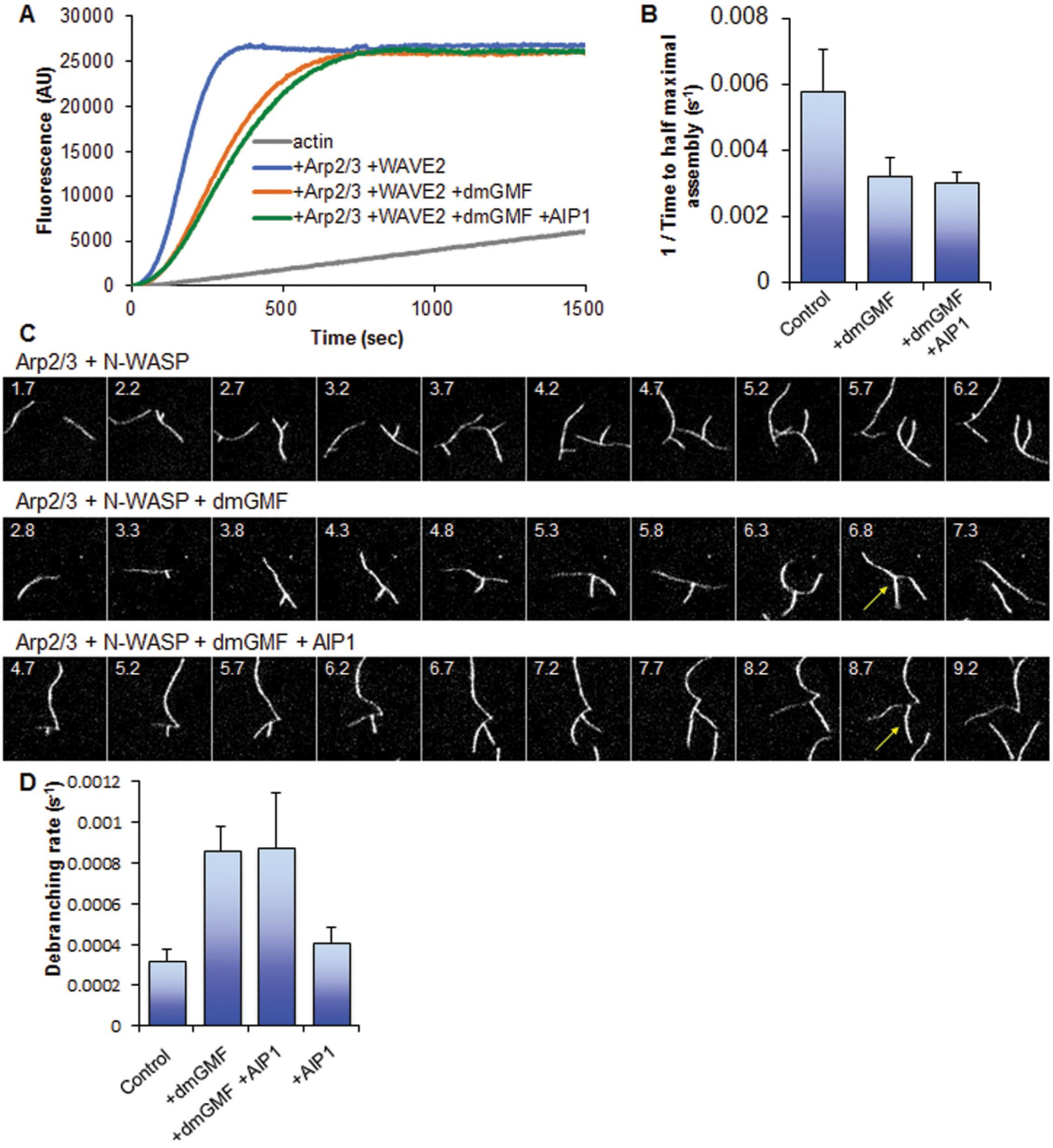

Figure S3. Aip1 does not affect Arp2/3-inhibition and de-branching activities of GMF *in vitro.*

Related to Figure 3.

(A) Inhibition of Arp2/3 complex-mediated actin assembly *in vitro* by *Drosophila* GMF (dGMF) in the presence of mouse AIP1. Reactions contained 2 µM actin monomers (5% pyrene-labeled), and as indicated: 20 nM bovine Arp2/3 complex, 200 nM human WAVE2 GST-VCA, 2 µM dGMF, and/or 1.5 µM AIP1. (B) Time to half-maximal polymerization for each curve in A was measured. Data are represented as mean ± SD. (C) TIRF microscopy analysis of actin filament debranching events monitored over time in reactions containing 1

μM actin monomers (10% OG-labeled), 5 nM bovine Arp2/3 complex, 100 nM bovine N-WASP GST-VCA, with or without 500 nM dGMF and/or 500nM mouse AIP1. Debranching events are marked by yellow arrows. Time is indicated in minutes. (D) Debranching rates shown for each condition were obtained by analyzing 51-70 branch points in each of three independent fields of view for a period of 15 min. Data are represented as mean ± SD.

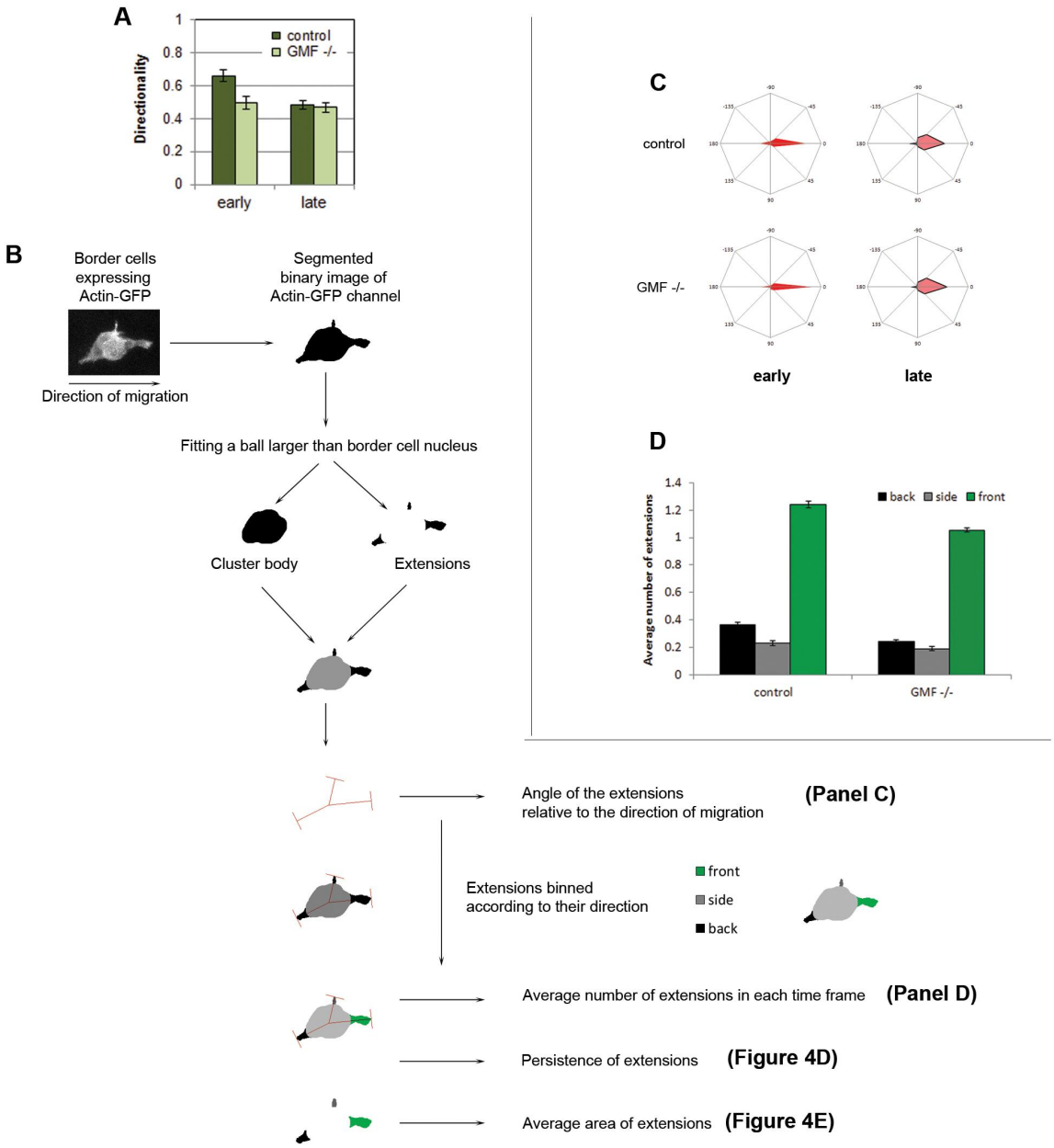

Figure S4. Analysis of border cell migration *in vivo*.

Related to Figure 4.

(A) In order to measure the directionality of border cell clusters, the net distance travelled by the border cell cluster (yellow line in Figure 4B) was divided by a path of a tracked single cell (blue line in Figure 4B). Data are represented as mean ± SEM. (B) Schematics of automatic procedure for defining border cells extensions. Cellular protrusions were automatically defined from projected GFP images of border cells cluster by custom made macros as described previously [S1]. Shortly, the projected GFP image of a border cell cluster was converted to binary image and image was segmented to represent the full outline

of the border cell cluster. The cluster body was defined as the area in which a circle slightly larger than border cell nucleus (diameter 9.45 μm) can be fitted in. Areas that are protruding outward the cluster body and exceed a minimum size of 3 μm^2 were defined as extensions and their direction and area were measured. Extensions were classified according to their direction as front (toward the oocyte and direction of migration: 0–45° and 315–360°), back (135–225°) and sideway (the rest) directions. In addition, extensions that were overlapping in subsequent time points were linked to measure their persistence. (C) Polar plot displaying angles of extension formed by control and GMF mutant border cell clusters. Note that both samples display clear bias of front extensions both in early and late phase, indicating that guidance cues are appropriately perceived. (D) Average number of extensions observed per each time frame during early phase migration is slightly reduced in GMF mutant border cells when compared to control cells. Data are represented as mean ± SEM.

SUPPLEMENTAL EXPERIMENTAL PROCEDURES

Plasmids

dGMF RE40543 full insert cDNA (*Drosophila* gold collection) was cloned into pENTRY-D/TOPO vector (Invitrogen). For generating GFP-dGMF, dGMF was thereafter cloned with NotI and AscI restriction enzymes into expression plasmid containing copper sulphate inducible pMT promoter and N-terminal GFP fusion. pMT plasmid [S2] was a kind gift from Duche Mullins, UCSF. Mouse GMFγ cDNA was cloned into pENTRY-D/TOPO vector (Invitrogen) according to manufacturer's instructions. GMFγ was subcloned to a destination vector containing CMV promoter and N-terminal EGFP fusion with Gateway cloning system (Invitrogen) according to manufacturer's protocol. For biochemical assays, coding sequences of full-length *Drosophila* GMF (dGMF), human WAVE2 VCA domain, and bovine N-WASP VCA domain were cloned into the NsiI and BamHI sites and EGFP-dGMF was cloned from pMT-EGFP-dGFP into NcoI and EcoRI sites of an *E. coli* GST-fusion expression vector, pGAT2 [S3].

Protein expression and purification.

GST-fusion proteins were expressed in *Escherichia coli* BL21 (DE3) cells by IPTG induction. GST-dGMF and GST-EGFP-GMF were purified from clarified cell lysates by glutathione affinity chromatography, and then treated with PreScission Protease or thrombin to remove GST, yielding untagged dGMF, respectively. EGFP-GMF was further purified with Superdex-200 gel filtration column (GE Healthcare). GST-VCA domains were purified by loading each lysate onto a 1 ml GST cartridge in a Profinia Protein Purification System (Bio-Rad), eluting with glutathione, and exchanging into a buffer lacking glutathione on a 10 ml De-salting cartridge. Bovine Arp2/3 complex was a kind gift from Brad Nolen (University of Oregon). Rabbit skeletal muscle actin was purified as described [S4]. To produce polyclonal rabbit antibodies (Storkbio Ltd), recombinant His-tagged dGMF was purified. GMF RE40543 full insert cDNA (*Drosophila* gold collection) was cloned into the HindIII-NcoI sites of pHAT [S3] vector with an N-terminal Histidine (6His)-tag. After induction, *E. coli* cells were harvested by centrifugation, resuspended in Lysis buffer (20 mM Tris-Hcl, pH 7.5, 150 mM NaCl, 10 mM Imidazole, 100 μM PMSF) and sonicated. Lysates were cleared by centrifugation, and recombinant His-tagged dGMF was purified using Ni-NTA Superflow Agarose beads (Sigma Aldrich), then desalted on a Sephadex 75 HiLoad gel filtration column (GE Healthcare). Protein was concentrated with 10kDa cut-off concentration tubes

(Millipore). To purify mouse AIP1, HEK293T cells were transiently transfected with pTT5SH8Q2-mAIP1 using 25 kDa linear polyethylenimine (Polysciences, Warrington, PA). Cells were harvested 72 h post-transfection and lysed by douncing and repeated freeze-thawing in 20 mM Tris/HCl pH 7.5, 150 mM NaCl, 1% (v/v) Triton X-100 and standard protease inhibitors. After extraction, the lysate was cleared by centrifugation and incubated with Ni^{2+}-NTA beads (Qiagen, Valencia, CA) for 90 min at 4°C in the presence of 10 mM imidazole. After washing with 20 mM Tris pH 7.5, 300 mM NaCl, 50 mM imidazole and 1 mM DTT, the proteins were eluted in washing buffer with 250 mM imidazole, and then concentrated and purified further on a Superose 6 gel filtration column (GE Healthcare Biosciences, Pittsburgh, PA) equilibrated in 20 mM Tris pH 8.0, 50 mM KCl and 1 mM DTT.

Actin Assembly Assays

Actin assembly assays (60 µl) contained 2 µM actin (5% pyrene labeled), 20 nM bovine Arp2/3 complex, 1.5 µM mouse AIP1, 200 µM WAVE2 GST-VCA, and the indicated concentrations of mGMF-γ or dGMF. After addition of initiation mix, polymerization kinetics were monitored in a fluorescence spectrophotometer (Photon Technologies International, Lawrenceville, NJ). The k_I was calculated using SciDavis software to fit the equation f(x)= (a*x)/(b+x) (where b=k_I) to the plot the time to half maximal polymerization for each concentration of dGMF.

TIRF Microscopy Assays for Actin Filament Debranching

TIRF microscopy debranching assays were performed using 1 µM actin, 10% Oregon-green labeled as described [S5], 5 nM bovine Arp2/3 complex, 100 nM N-WASP GST-VCA, and 500 nM dGMF and/or 500 nM mouse AIP1. Movies were recorded on a Nikon-Ti2000 microscope (described in [S6]) starting 2 min and 30 s after reaction initiation at 10 s intervals for 15 min using 200 ms exposures. Debranching rates were calculated as described [S6]. Only branches that formed stable y-junctions for at least 30s were included in the analysis.

Affinity purification of antibodies

IgG fractions of rabbit sera immunized with His-tagged dGMF were purified by affinity chromatography on beads coated with His-tagged dGMF. 500 µl fractions of IgGs were

eluted from the antigen-coated beads with 100 mM glycine pH 2.6 and immediately neutralized with 15 µl 3M Tris-HCl pH 8.8 and 17 µl 3M NaCl. Correct fractions were identified by Western blot analysis of fly extracts using *gmf*^{1} mutant extract as a control. Fresh aliquots of the purified antibody were incubated with *gmf*^{1} mutant fly ovarioles at +4 ^{o}C overnight prior to immunostainings to remove non-specific antibodies.

Cell culture and RNAi

Drosophila S2R+ and S2 (Invitrogen) cells were cultured at 24°C in a humidified incubator in Schneider's medium (Invitrogen) supplemented with 10% heat-inactivated FBS (GIBCO) and antibiotics (50 U/ml penicillin and 50 µg/ml streptomycin; GIBCO). For generation of RNAi, gene-specific sequences based on the DRSC validation library (http://flyrnai.org) were amplified from either from *Drosophila* gold collection cDNA clones or from S2R+ cells by PCR with gene-specific primers GMF-RNAi1 (DRSC01928), GMF-RNAi2 (DRSC35400), Aip1-RNAi (DRSC09787), and ArpC5-RNAi (DRSC00730) containing the T7-binding site. As RNAi control, 900 bp sequence, not present in the fly genome, was amplified from the pBluescript SK plasmid [S7]. Double-stranded RNA (dsRNA) was synthesized using the MEGAscript T7 Kit (Invitrogen) and purified with NucAway Spin columns (Applied Biosystems). Gel electrophoresis was used to confirm the integrity of the dsRNAs and dsRNAs were quantified by using NanoDrop spectrometry. For measuring lamellipodial width upon GMF silencing, S2R+ cells were plated on 24-wells and mixed with 2 µg of dsRNA. Cells were grown for 3–4 d at 24°C, depending on the experiment, re-plated onto Con A–coated circular 13 mm diameter coverslips and allowed to spread before analysis (typically 1–3 h). The silencing of GMF was verified by Western blotting of cellular lysates and by immunofluorescence microscopy. Mouse B16-F1 cells were maintained at 37ºC in humidified atmosphere (5% CO2) in Dulbecco's modified Eagle's medium (DMEM) supplemented with 10% fetal bovine serum (Hyclone), 2 mM L-glutamine, penicillin, and streptomycin (Sigma-Aldrich). HEK293T cells, used for expression of mouse Aip1, were maintained at 37°C under a humidified atmosphere containing 5% CO_2 in Dulbecco's modified Eagle's medium (DMEM), supplemented with 10% (v/v) heat-inactivated foetal bovine serum, glucose (4.5 g/l), penicillin (100 units/ml) and streptomycin (100 µg/ml).

Live imaging of lamellipodial dynamics

For live imaging of dGMF dynamics in lamellipodia, S2 cells (Invitrogen) were cultured on 24-well plates until 50% confluent. Cells were transfected with 0.2 μg of plasmid DNA using Effectene transfection reagent (Qiagen) according to the manufacturer's instructions. GFP-tagged GMF under the control of a metallothionein promoter (pMT) was used in these experiments. GFP-GMF expression was induced by addition of 300 nM copper sulphate solution 1 day before live imaging. Cells were plated on Concanavalin A-coated glass-bottomed dishes (MatTek Corporation) and left to spread for 1-3 h until imaged. Transient transfection of B16-F1 cells was performed with FugeneHD (Roche) transfection reagent according to the manufacturer's instructions. One μg of the desired plasmid (GFP-GMFγ and Actin-Cherry) was used per dish. Human pCherry-ß-actin plasmid was a gift from M. Bähler (Westfalian Wilhelms-University, Münster, Germany). After transient transfection, cells were incubated for 24 h and prior to live imaging re-plated on 25 μg/ml laminin-coated glass-bottomed dishes (MatTek Corporation). Immediately prior to imaging, lamellipodia formation was induced by adding 50 μM $AlCl_3$ and 30 mM NaF [S8]. The time-lapse images were acquired with a 3I Marianas imaging system (3I intelligent Imaging Innovations), with 63x/1.2 W C-Apochromat Corr WD=0.28 M27 objective (Zeiss) and appropriate filters. Imaging of S2 cells was done at room temperature, and imaging of B16 cells was done using a heated environment (37°C) with CO_2. Images were acquired using a Neo sCMOS (Andor) camera and SlideBook 5.5 software (3I intelligent Imaging Innovations). Kymographs were generated using ImageJ from time lapse sequences along 1 pixel wide lines oriented perpendicular to the cell periphery (in the case of S2 cells) or lamellipodial edge (for B16 cells). Fluorescence intensity of GFP-GMF and/or Actin-Cherry during each protrusion and retraction was measured from a straight line along the leading edge of the cell.

Immunofluorescence staining

Cells were fixed with 4% formaldehyde in PBS for 20 min at room temperature, permeabilized with 0.1% Triton X-100 in PBS (PBT) and blocked for 30 min in 2.5% BSA-PBT. Cells were stained with primary antibodies: anti-dGMF 1:50, anti-GMFγ (Proteintech) 1:100. After 1 h at room temperature, cells were washed several times with 2.5% BSA-PBT for 2 h at room temperature. Cells were treated with secondary antibodies together with fluorochrome conjugated phalloidin (Invitrogen) and 4',6-diamidino-2-phenylindole (DAPI) for 1 h at room temperature, and washed with several changes of PBT, 2 h each. Glasses were rinsed with dH_2O and mounted by using aqueous fluorescent mounting medium (DAKO) and

imaged with a Zeiss Imager M2 fluorescence microscope equipped with an Axio Cam HRm camera and AxioVision software using a PlanApo 63x/1.40 (oil) objective. For RNAi experiments, images were acquired using the same exposure time. The width of lamellipodia in S2R+ cells was manually measured as a width of a bright Phalloidin-stained area encircling the periphery of the cell from 2-3 locations of the cell, minimum of 30 cells were measured for each sample. F-actin accumulation upon RNAi silencing was quantified by scoring the cells with 'none' (absence of visible actopic actin dots in cells cortex or cytoplasma), 'weak to moderate' (ectopic actin dots visible in cytoplasma and in cell cortex) or 'strong' (large and bright actin aggregates visible both in cell cortex and cytoplasma) F-actin accumulation phenotypes. Samples were scored blindly. Ovaries were dissected in Schneider medium (Gibco) with 0.5 µM insulin (Sigma) and fixed in 4% para-formaldehyde (Electron Microscopy Sciences) for 20 minutes, permeabilized with PBT and blocked for 30 min in 2.5% BSA-PBT. Anti-GMF, fluorochrome donjugated Phalloidin and DAPI stainings was done using standard procedures as described above. Images were acquired on a Leica TCS SP5 confocal microscope using an HCX APO 63x/1,30 Corr (glycerol) CS 21 objective.

Western blotting

S2R+ cells were collected and lysed for 30 min on ice in 30 mM Tris-HCl pH 7.5, 150 mM NaCl, 1% Triton X-100, 10% glycerol, 1mM PMSF, supplemented with protease inhibitor cocktail (Roche). Cell debris was cleared by centrifugation, and protein concentration was determined with Bradford reagent. Equal amounts of protein from each sample were run on 15% SDS-PAGE gels, and the efficiency of the knock-down was analyzed by Western blotting with anti-dGMF, anti-twinfilin [S9], anti-cofilin (a kind gift from Dr. James R. Bamburg), anti-Aip1 [S10] (a kind gift from Dr J. Chen) and anti-tubulin (DM1A, Sigma) and detected with chemiluminescent ECL reagent.

Drosophila strains and genetics

Drosophila husbandry was performed by standard procedures at 25°C. Fly strains P{EP}CG5869(G2885), c306-*GAL4,* UAS-Arcp1-GFP and UAS-Dia-CA flies were obtained from the Bloomington Stock Center. RNAi lines UAS-Aip1-RNAi-GD (transformant id: 22851), UAS-AIP1-RNAi-kk (transformant id: 108442), UAS-GMF-RNAi-kk (transformant id: 101994) were obtained from Vienna RNAi *Drosophila* Stock Center. 2xslbo-Actin-GFP (slbo border cell enhancer promoter driven Actin-GFP) was used to mark border cell cluster for live imaging experiments as described [S11]. UAS-Arcp1-GFP has been described [S12].

dGMF mutants were generated by imprecise excision of the G2885 EP element. Deletion in the *dGMF* locus was verified by analyzing genomic DNA by PCR and its molecular nature was determined by sequencing the PCR product. For border-cell–specific RNAi expression, Gal4/UAS system was used [S13]. Flies were incubated 2 days at either at 25°C or 29°C before dissection of the ovaries. For ubiquitous expression of dGMF, Tub-Gal4/cg5869 EPG2885 and control Tub-Gal4/w1118 larvae were picked as first instar and grown on standard food for 72h (96h AEL). Total RNA was isolated with Nucleospin RNA II kit (Macherey-Nagel) and reverse transcribed with Revertaid cDNA synthesis kit (Thermo Scientific) according to manufacturer's protocols. qPCR was performed with SYBR green technology and relative cg5869 mRNA levels were calculated using rp49 as a reference gene. The primers used were rp49 forward AGGGTATCGACAACAGAGTG, rp49 reverse CACCAGGAACTTCTTGAATC, cg5869 forward GGGCCGTTGTCAAAAGCAAT, cg5869 reverse ATGCATCGTTGGTATCGGCT.

Live imaging of border cell migration and data analysis

Live imaging of border cell migration was performed as described [S1, S14]. Note that due to the genetic background and/or minor differences in culturing or imaging conditions, quantified features in control may differ slightly from the earlier published data. Thus, control was carefully repeated to analyze the situation in this particular genetic background and to be able to compare it with GMF mutants in the same genetic background. Images were acquired using an SP5 (Leica) confocal microscope with 63x objective equipped with sensitive HyD detector. Z sections of migrating border cell clusters were captured 1.5 μm apart, at 60-120 s intervals. Timelapse movies were assembled and analysed using ImageJ and customized macros as described [S1].

Statistics

Statistical significance was determined with unpaired Student's t-test with unequal variance. All quantitative data are presented as mean ± SEM. *P* values were from the two-tailed test.

SUPPLEMENTAL REFERENCES

S1. Poukkula, M., Cliffe, A., Changede, R., and Rørth, P. (2011). Cell behaviors regulated by guidance cues in collective migration of border cells. J. Cell. Biol. *192*, 513-524.

S2. Iwasa, J.H., and Mullins, R.D. (2007). Spatial and temporal relationships between actin-filament nucleation, capping, and disassembly. Curr. Biol. *17*, 395-406.

S3. Peränen, J., Rikkonen M., Hyvönen, M., and Kääriäinen, L.(1996). T7 vectors with modified T7lac promoter for expression of proteins in Escherichia coli. Anal. Biochem. *236*, 371-373.

S4. Pollard, T.D., and Cooper, J.A. (1984). Quantitative analysis of the effect of Acanthamoeba profilin on actin filament nucleation and elongation. Biochemistry. *23*, 6631-6641.

S5. Breitsprecher, D., Jaiswal, R., Bombardier, J.P., Gould, C.J., Gelles, J., and Goode, B.L. (2012). Rocket launcher mechanism of collaborative actin assembly defined by single-molecule imaging. Science. *336*, 1164-1168.

S6. Ydenberg, C.A., Padrick, S.B., Sweeney, M.O., Gandhi, M., Sokolova, O., and Goode, B.L. (2013). GMF Severs Actin-Arp2/3 Complex Branch Junctions by a Cofilin-like Mechanism. Curr. Biol. *23*, 1037-1045.

S7. Rogers, S.L., and Rogers, G.C. (2008). Culture of Drosophila S2 cells and their use for RNAi-mediated loss-of-function studies and immunofluorescence microscopy. Nat. Protoc. *3*, 606-611.

S8. Hahne, P., Sechi, A., Benesch, S., and Small, J.V. (2001). Scar/WAVE is localised at the tips of protruding lamellipodia in living cells. FEBS Lett. *492*, 215-220.

S9. Wahlström, G., Vartiainen, M., Yamamoto, L., Mattila, P.K., Lappalainen, P., and Heino, T.I. (2001). Twinfilin is required for actin-dependent developmental processes in Drosophila. J Cell Biol. *155*, 787-796.

S10. Chu, D., Pan, H., Wan, P., Wu, J., Luo, J., Zhu, H., and Chen, J. (2012). AIP1 acts with cofilin to control actin dynamics during epithelial morphogenesis. Development. 139, 3561-3571.

S11. Fulga, T.A., and Rørth, P. (2002). Invasive cell migration is initiated by guided growth of long cellular extensions. Nat. Cell Biol. *4*, 715-719.

S12. Hudson, A.M., and Cooley, L. (2002). A subset of dynamic actin rearrangements in Drosophila requires the Arp2/3 complex. J. Cell Biol. *156*, 677-687.

S13. Brand, A.H., and Perrimon, N. (1993). Targeted gene expression as a means of altering cell fates and generating dominant phenotypes. Development. *118*, 401-415.

S14. Bianco, A., Poukkula, M., Cliffe, A., Mathieu, J., Luque, C.M., Fulga, T.A., and Rørth, P. (2007). Two distinct modes of guidance signalling during collective migration of border cells. Nature. *448*, 362-365.